Published March 1, 1966

Studies on Ion Accumulation in Muscle Cells

GILBERT NING LING and MARGARET MARY OCHSENFELD

From the Department of Molecular Biology in the Department of Neurology, Division of Medicine, Pennsylvania Hospital, Philadelphia

ABSTRACT A comparison is made between the quantitative predictions of equilibrium ionic distribution in living cells according to the membrane theory (Donnan equilibrium) and according to the association-induction hypothesis. This comparison shows that both theories predict competitive effects of one permeant ion on the equilibrium concentration of another permeant ion; but within the limit of experimental accuracy only the association-induction model predicts quantitatively significant specific competition of one specified ion with the accumulation of another specified ion. The equilibrium distributions of K^+, Rb^+, and Cs^+ ions in frog sartorius muscle were studied and quantitatively significant specific competition was demonstrated; these results favor the association-induction hypothesis (adsorption on cell proteins and protein complexes and partial exclusion from cell water). Based on this model we estimated that at 25°C, the apparent association constants for K^+, Rb^+, and Cs^+ ion are 665, 756, and 488 $(mole/liter)^{-1}$. We found that the total concentration of adsorption sites (no less than 240 mmole/kg of fresh cells) agrees with the analytically determined concentrations of β- and γ-carboxyl groups of muscle cell proteins (260 to 288 mmole/kg).

INTRODUCTION

Ions and other solutes do not, as a rule, distribute themselves within cells at the concentrations anticipated on the basis of simple thermodynamic equilibria (1, 2). Past study of this phenomenon has often been hampered by difficulties in preserving isolated cells in reasonably good condition for a prolonged period of time. Recently, by adapting tissue culture methods, we have overcome this problem and have been able to investigate quantitatively the steady ionic level reached in the muscle cell following changes of the external ionic environment.

A priori, a constantly maintained level of an ion or other solute in the cell may represent either an equilibrium phenomenon or a steady-state phenomenon. The maintenance of an equilibrium needs no expenditure of free energy. However, in the maintenance of a steady state, which must involve active transport or "pumps" of some sort, a continued free energy expenditure is mandatory. Comparison of the total energy available to the muscle cell

Downloaded from jgp.rupress.org on December 16, 2012

Published March 1, 1966

with the energy need of a *consistent* (in contrast to an *ad hoc*) active transport model for maintaining the solute distribution led to the conclusion that such a model is against the second law of thermodynamics (3, 4). Since there is no third alternative, the constant level of an ion or solute within the cell must represent an equilibrium phenomenon. In the present communication, the experimental data obtained are compared with the quantitative predictions of two equilibrium models: (*a*) the classical Donnan membrane theory (5, 6; see also Boyle and Conway in reference 1) and (*b*) the association-induction hypothesis (3).

THEORY

The Membrane Theory

If we interpose a membrane between two aqueous phases and introduce a monovalent ionic substance that cannot pass through the membrane into one phase, the distribution of the permeant monovalent ions must follow a set pattern. Thus, if the impermeant ion is an anion, represented as R^- (its concentration is $[R^-]$), and if there are two permeant cations (p_i^+ and p_j^+) and one permeant anion (p_k^-),

$$\frac{[p_i^+]_{in}}{[p_i^+]_{ex}} = \frac{[p_j^+]_{in}}{[p_j^+]_{ex}} = \frac{[p_k^-]_{ex}}{[p_k^-]_{in}} = r \tag{1}$$

where r is the Donnan ratio; $[p_i^+]_{in}$, the equilibrium concentration of the ith monovalent cation in the phase referred to as the inside phase; and $[p_k^-]_{ex}$, the equilibrium concentration of the kth anion in the external phase. The jth monovalent cation, p_j^+, represents a cation distinguishable from the ith ion by chemical or physical (e.g., radioactivity) means. Since macroscopic electroneutrality must be maintained,

$$[p_j^+]_{ex} + [p_i^+]_{ex} = [p_k^-]_{ex}, \tag{2}$$

and

$$[p_j^+]_{in} + [p_i^+]_{in} = [p_k^-]_{in} + [R^-]. \tag{3}$$

From Equations 1, 2, and 3

$$[p_i^+]_{in} = \frac{[p_i^+]_{ex}\left([R^-] + \sqrt{[R^-]^2 + 4[p_k^-]_{ex}^2}\right)}{2[p_k^-]_{ex}}. \tag{4}$$

When $4[p_k^-]^2 \ll [R^-]^2$,

$$\frac{1}{[p_i^+]_{in}} = \frac{[p_j^+]_{ex}}{[p_i^+]_{ex}[R^-]} + \frac{1}{[R^-]}. \tag{5}$$

Downloaded from jgp.rupress.org on December 16, 2012

Published March 1, 1966

Thus, within the restriction mentioned, one should obtain a linear relation between $\frac{1}{[p_i^+]_{in}}$ and $\frac{1}{[p_i^+]_{ex}}$ for each constant value of $[p_j^+]_{ex}$. The family of lines, each corresponding to a different value of $[p_j^+]_{ex}$, tends to converge toward the same locus on the ordinate.

In Fig. 1, $[p_i^+]_{ex}$ is plotted against $[p_i^+]_{in}$ in the presence of varying concen-

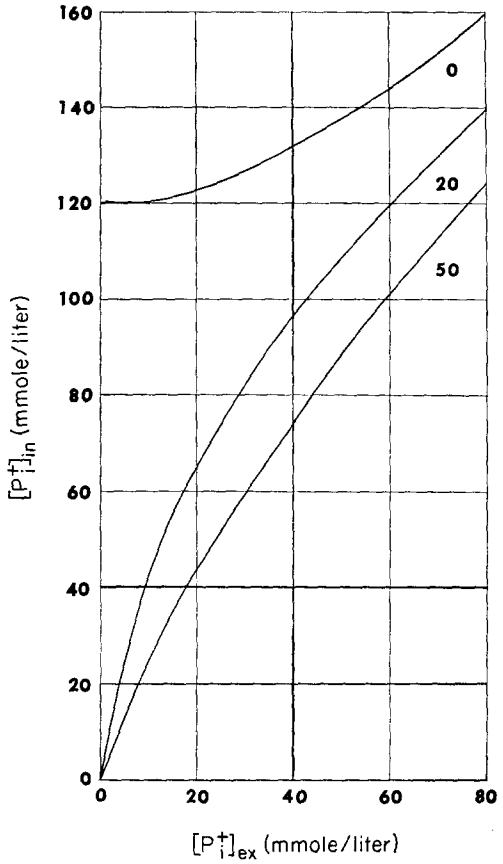

FIGURE 1. Theoretical relation between $[p_i^+]_{ex}$ and $[p_i^+]_{in}$ in the presence of varying concentrations of $[p_j^+]_{ex}$ (at 0, 20, and 50 mmole/liter concentration) according to the Donnan membrane equilibrium. Concentration of impermeant anion, R^-, 120 mmole/liter.

trations (0, 20, and 50 mmole/liter) of $[p_j^+]_{ex}$ according to Equation 4. In Fig. 2, we have plotted the reciprocals of $[p_i^+]_{in}$ against the reciprocals of $[p_i^+]_{ex}$ also according to Equation 4.[1] $[R^-]$ is 120 mmole/liter in this model. From the lowermost curve ($[p_j^+] = 0$), one can recover a reasonably accurate value of $[R^-]$.

We may write Equation 5 in terms of activities rather than concentrations.

[1] The impression, that the linear relationship and the common intercept apply over the entire range of $[p_i^-]_{ex}$ values without restriction, arises from the much greater influence exercised by the points in the lower concentration range on the over-all shape of the reciprocal plot. The relationship does not hold at points close to the origin as the curved portions of the lines show.

Downloaded from jgp.rupress.org on December 16, 2012

Published March 1, 1966

Thus, if the activity of the jth external cation is written as $[a_j^+]_{ex}$ and that of the ith intracellular cation as $[a_i^+]_{in}$ then

$$[a_i^+]_{in} = \gamma_i^{in}[p_i^+]_{in}, \quad (6)$$

$$[a_j^+]_{ex} = \gamma_j^{ex}[p_j^+]_{ex}, \quad (7)$$

and so on, where γ_i^{in} and γ_j^{ex} are the corresponding activity coefficients.

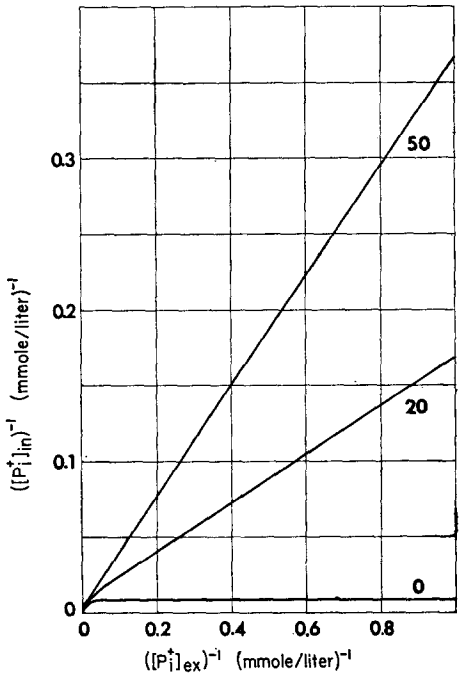

FIGURE 2. Theoretical relation between the reciprocals of $[p_i^+]_{ex}$ and $[p_i^+]_{in}$ in the presence of varying $[p_j^+]_{ex}$ (0, 20, and 50 mmole/liter) according to the Donnan membrane equilibrium. Data are the same as in Fig. 1.

Equation 5 then becomes

$$\frac{1}{[p_i^+]_{in}} = \frac{\gamma_i^{in}\gamma_j^{ex}}{\gamma_R\gamma_i^{ex}} \cdot \frac{[p_j^+]_{ex}}{[p_i^+]_{ex}[R^-]} + \frac{\gamma_i^{in}}{\gamma_R[R^-]}, \quad (8)$$

where γ_R and γ_i^{ex} are the activity coefficients of R and the external ith cation respectively.

Thus in the Donnan system, there is competition between p_i^+ and p_j^+ ; in this system there is also a certain degree of specificity determined by the differences in the activity coefficients. However, at the concentration found in cells (e.g., 0.1 mole/liter), the activity coefficients of alkali metal ions are in general not very far apart (i.e., for chloride salts, Cs^+, 0.754; Rb^+, 0.764; K^+, 0.770; Na^+, 0.778; see reference 7). The maximum difference between any pair of alkali metal ions is less than 2% (and is thus below the limit of experimental error).

Downloaded from jgp.rupress.org on December 16, 2012

Published March 1, 1966

Thus, within the resolving power of the present experimental accuracy, any monovalent cation, p_j^+, at, say 20 to 50 mmole/liter, should have the same effect on the equilibrium intracellular concentration of p_i^+, so long as the ith ion is a monovalent cation.

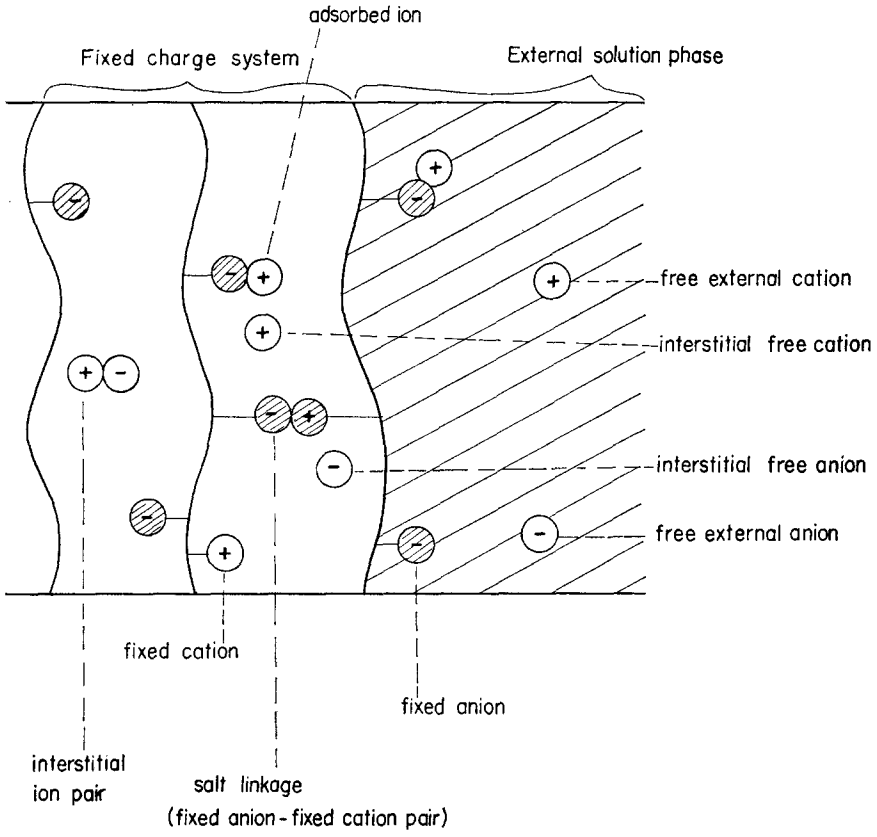

FIGURE 3. Diagram of a fixed charge system in contact with a free solution phase.

Association-Induction Hypothesis

In the association-induction hypothesis (3, 4, 8), the living cell is represented as a proteinaceous fixed charge system. The cell proteins form a charge-bearing, three dimensional network, onto which are adsorbed ions and non-electrolytes, as well as other molecules, minor in amount but essential in function. The protein matrix also polarizes and orients the successive layers of water molecules which fill the spaces between the protein chains. Such a fixed charge system is diagrammatically illustrated in Fig. 3. In the external solution, the ith cation exists only in the free form. Within the fixed charge system, however, it may assume one of three forms: (*a*) interstitial free cation, (*b*) interstitial ion pair, (*c*) adsorbed ion. For simplicity of presentation, we shall

Downloaded from jgp.rupress.org on December 16, 2012

Published March 1, 1966

ignore the interstitial ion pairs, considering these as quantitatively trivial. Denoting the percentage of water in the cell as α (in liters per kilogram of fresh cells),

$$[p_i^+]_{in} = \alpha[p_i^+]_{ins} + [p_i^+]_{ad}. \quad (9)$$

The successive terms refer to the total intracellular ith cation, the interstitial free ith cation, and the adsorbed ith cation respectively. $[p_i^+]_{in}$ and $[p_i^+]_{ad}$ are in moles per kilogram of fresh cells; $[p_i^+]_{ins}$ is in moles per liter of intracellular water. Leaving the presentation of a *general equation* to another forthcoming theoretical paper (for brief account, see reference 8), we shall forthwith present in its simplified form the *special equation* for the intracellular distribution of the ith monovalent cation. In the case to be considered here, the various adsorption sites have association constants (for the ith and the jth cation) not too far apart, and the ith ion association constants for adsorption on these different sites are not too far apart from each other. The justification for these criteria appears in the section on experimental results. Under these conditions, Equation 9 assumes the following form:

$$[p_i^+]_{in} = \alpha q_{i(k)}^{\infty \to ins}[p_i^+]_{ex} + \frac{[f^-]^{total}\tilde{K}_{i(k)}^{\infty \to T}[p_i^+]_{ex}}{1 + \tilde{K}_{i(k)}^{\infty \to T}[p_i^+]_{ex} + \tilde{K}_{j(k)}^{\infty \to T}[p_j^+]_{ex}}. \quad (10)$$

This is the special equation according to the association-induction hypothesis for selective ion accumulation without cooperative interaction (reference 3, chapter 5; references 8 to 10). $q_{i(k)}^{\infty \to ins}$ is the mean equilibrium distribution coefficient of the ith cation between the intracellular water and the extracellular water; the migration of the ith (and jth) cation in and out of the cells is accompanied by the kth anion. $\tilde{K}_{i(k)}^{\infty \to T}$ and $\tilde{K}_{j(k)}^{\infty \to T}$ are the mean apparent *association* constants of the ith and jth monovalent cations respectively on (all) the anionic sites. T is the general symbol for all the fixed anions in the system. The apparent association constant differs from the true association constant by a factor corresponding to cations that also compete for the same anionic sites but are, for convenience or other reasons, not explicitly dealt with (e.g., H^+ ion, fixed cations). $[f^-]^{total}$ is the total intracellular concentration of anionic sites in moles per kilogram of fresh cells.

Criteria for the Experimental Testing of the Membrane Theory and the Association-Induction Hypothesis

An extensive discussion of the value of $q_{i(k)}^{\infty \to ins}$ and its molecular interpretation will be the subject of a succeeding paper (for a brief discussion, see references 4, 11, and 12). It is sufficient to mention that as a rule, $\alpha q_{i(k)}^{\infty \to ins}$ is less than 0.2 for frog sartorius muscle cells. Anticipating the results of the experimental studies to be given below, showing $[p_i^+]_{ad}$ (for K^+, Rb^+, and Cs^+) $\gg$

Downloaded from jgp.rupress.org on December 16, 2012

Published March 1, 1966

($\alpha\ q_{i(k)}^{\infty \to ins}\ [p_i^+]_{ex}$) (see Discussion), we can ignore the interstitial ions. Equation 10 simplifies to

$$[p_i^+]_{in} = \frac{[f^-]^{total} \bar{K}_{i(k)}^{\infty \to T} [p_i^+]_{ex}}{1 + \bar{K}_{i(k)}^{\infty \to T} [p_i^+]_{ex} + \bar{K}_{j(k)}^{\infty \to T} [p_j^+]_{ex}} \tag{11}$$

Defining $K_{i(k)}^{\infty \to T}$, $K_{j(k)}^{\infty \to T}$ as the mean apparent *dissociation* constants for the ith and jth cation respectively we have

$$K_{i(k)}^{\infty \to T} = \frac{1}{\bar{K}_{i(k)}^{\infty \to T}}, \tag{12}$$

and

$$K_{j(k)}^{\infty \to T} = \frac{1}{\bar{K}_{j(k)}^{\infty \to T}}. \tag{13}$$

The reciprocal form of Equation 11 is:

$$\frac{1}{[p_i^+]_{in}} = \frac{K_{i(k)}^{\infty \to T}}{[f^-]^{total}} \left(1 + \frac{[p_j^+]_{ex}}{K_{j(k)}^{\infty \to T}}\right) \frac{1}{[p_i^+]_{ex}} + \frac{1}{[f^-]^{total}} \tag{14}$$

Thus, if $\frac{1}{[p_i^+]_{in}}$ is plotted against $\frac{1}{[p_i^+]_{ex}}$ with a fixed concentration of the competing ion, $[p_j^+]_{ex}$, one should obtain a straight line. Furthermore, the intercepts on the ordinate for a family of curves with different concentrations of competing ions should meet at the same locus; this locus should be the reciprocal of the total concentration of fixed anionic sites in the system. Figs. 4 and 5 show linear and reciprocal plots of $[p_i^+]_{in}$ against $[p_i^+]_{ex}$ in the presence of varying concentrations (0, 20, 50 mmole/liter) of the jth competing ion. These theoretical curves were computed on the basis of a population with an equal mixture of two types of sites (each 60 mmole/kg in concentration). The association constant for the ith ion is twice as high for one type of site as for the other.[2] Note that the reciprocal plot yields an accurate value of the total fixed anionic site concentration when there is no competing ion present even when the sites are not all the same. The $K_{i(k)}^{\infty \to T}$ obtained in such a case is a weighted average.

In the case when ($\bar{K}_{i(k)}^{\infty \to T}\ [p_i^+]_{ex}$) and ($\bar{K}_{i(k)}^{\infty \to T}\ [p_j^+]_{ex}$) are both considerably larger than unity, Equation 10 simplifies to:

$$[p_i^+]_{in} = \frac{[f^-]^{total}\ \bar{K}_{j(k)}^{\infty \to T}\ [p_i^+]_{ex}}{\bar{K}_{i(k)}^{\infty \to T}\ [p_i^+]_{ex} + \bar{K}_{j(k)}^{\infty \to T}\ [p_j^+]_{ex}}. \tag{15}$$

[2] The values of the parameters used here correspond roughly to those from our experimental studies to be described below.

Downloaded from jgp.rupress.org on December 16, 2012

Published March 1, 1966

When the ith ion is labeled with a radioisotope and the jth is nonlabeled ion of the same chemical species (e.g., nonlabeled K^+ ion competing against K^{42}-labeled K^+ ion), $\tilde{K}_{i(k)}^{\infty \to T} = \tilde{K}_{j(k)}^{\infty \to T}$. Equation 14, in reciprocal form, simplifies to

$$\frac{1}{[p_i^+]_{in}} = \frac{[p_j^+]_{ex}}{[p_i^+]_{ex} \cdot [f^-]^{total}} + \frac{1}{[f^-]^{total}}. \quad (16)$$

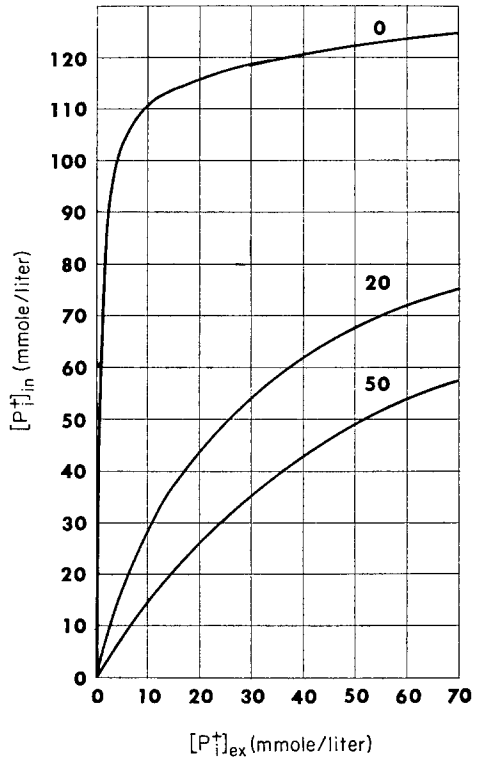

FIGURE 4. Theoretical relation between $[p_i^+]_{in}$ and $[p_i^+]_{ex}$ in the presence of varying concentrations of $[p_j^+]_{ex}$ (0, 20, and 50 mmole/liter), according to the association-induction hypothesis. $\alpha q_{(k)}^{\infty \to ins}$ here has the value of 0.2. The concentration of each of the two types of fixed anion sites was 60×10^{-3} mole/kg. The association constant for the jth ion is 10^3 for both types of sites; those for the ith ion are 10^3 and 2×10^3 respectively.

This equation is analogous in form to Equation 5, with the total concentration of fixed anionic sites, $[f^-]^{total}$, replacing the concentration of impermeant anion, $[R^-]$, in the Donnan system.

Thus, under the special conditions when $\tilde{K}_{i(k)}^{\infty \to T} = \tilde{K}_{j(k)}^{\infty \to T}$ and $(\tilde{K}_{i(k)}^{\infty \to T}\,[p_i^+]_{ex})$, $(\tilde{K}_{j(k)}^{\infty \to T}\,[p_j^+]_{ex}) \gg 1$, the model according to the association-induction hypothesis approaches the same limiting relation as the Donnan system, when $[R^-] \gg ([p_i^+]_{ex} + [p_j^+]_{ex})$. However, when $\tilde{K}_{i(k)}^{\infty \to T}$ is not equal to $\tilde{K}_{j(k)}^{\infty \to T}$, the behavior of the two models becomes totally different. According to the Donnan equilibrium, the effect of a competing monovalent cation (the jth) on the equilibrium concentration of another monovalent cation (ith) is (within the experimental accuracy of the present work) indifferent to the nature of both the ith and jth ion. According to the association-induction hypothesis, a difference in the nature of the ith or jth ion may produce significantly different

Downloaded from jgp.rupress.org on December 16, 2012

Published March 1, 1966

degrees of competition. Thus the crucial test consists of a *comparison of the effects of the same jth cation on the accumulation of two different radioactively labeled ith cations.*

MATERIALS AND METHODS

Sartorius muscles of medium sized (ca. 40 g) leopard frogs (*Rana pipiens*, Schreber) were used for all the experiments presented in this paper. Since a large number of

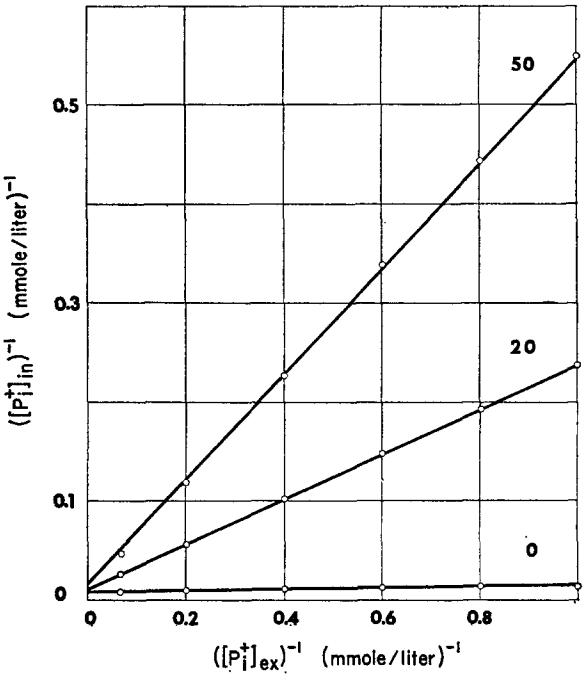

FIGURE 5. Theoretical relation between the reciprocal of $[p_i^+]_{ex}$ and $[p_i^+]_{in}$ in the presence of varying concentrations of $[p_j^+]_{ex}$ (0, 20, and 50 mmole/liter) according to the association-induction hypothesis. Points are calculated on the basis of the data given in Fig. 4; lines are calculated from these points by the method of least squares. The intercept of the lowest curve is 0.00833 (mmole/liter)$^{-1}$, which gives the correct concentration of the total fixed anions as 120 mmole/liter.

frogs had to be sacrificed each time, we could not follow the strict criteria for choosing healthy frogs described earlier (reference 3, Appendix G). All animals that were outwardly healthy were used. In general, three sartorius muscles from three different frogs were weighed individually on a torsion balance (initial weight), tied with small bits of colored thread, and introduced into test tubes containing 10 ml of the experimental solutions to be described. The test tubes, stoppered and sealed with Parafilm, were mounted on a rotor tilted at a 45° angle which turned at the rate of five rotations per minute. The temperature of the room varied between 23° and 26°C.

In studying Na^+ ion distribution, 100 ml of experimental solution was used for

Downloaded from jgp.rupress.org on December 16, 2012

Published March 1, 1966

each group of muscles, and the Erlenmeyer flasks containing the solution were shaken in an Aminco constant temperature bath (25° ± 0.05°C) at the rate of ninety oscillations per minute, each full excursion measuring 1 in.

At the end of the incubation period, the muscles were blotted on damp filter paper, weighed again (final weight), and introduced into 1.2 cm (diameter) × 14 cm Lusteroid tubes (Lusteroid Container Co., Maplewood, N.J.); 1 ml 1 N HCl was added. After 12 hr during which the distribution of the isotope in the HCl solution reached equilibrium, the radioactivity in the HCl solution, together with that in the tissue was assayed in the same Lusteroid tube using a γ-scintillation–well counter and scaler (Packard). To find the specific activity of the isotope, a 1 ml sample of the bathing solution, either as such or after suitable dilution, was also assayed. In general, each sample counted more than 4,000 CPM.

We determined nonlabeled Na^+ ion concentration by flame photometry (Beckman DU spectrophotometer) on a 0.1 N HCl extract of the tissue and using 0.1 M KH_2PO_4 as "radiation buffer" (reference 3, p. 201).

The experimental solutions were modified Ringer's bicarbonate solutions which we had saturated with a 5% CO_2-95% O_2 mixture (see reference 3, Appendix H). There were two general types of experimental solution:

1. The first was used for experiments lasting no longer than 25 hr; these solutions contained: $MgSO_4$ (1.2 mmole/liter), $CaCl_2$ (0.72 mmole/liter), $NaHCO_3$ (17.3 mmole/liter), NaH_2PO_4 (2.0 mmole/liter), Na_2HPO_4 (1.2 mmole/liter), and glucose (24.0 mmole/liter) in addition to the components shown in Table I. The pH was approximately 7.3–7.4.

As a rule we used the acetates of K, Rb, and Cs rather than the chlorides because the data from the acetate experiments, while not differing from the chloride experiments in any fundamental way, are more quantitatively consistent.

2. The second type of solution was used in studies of ionic accumulation over periods longer than 25 hr. In addition to the components shown in Table I, part ii, these solutions contained $MgSO_4$ (1.0 mmole/liter), $CaCl_2$ (0.72 mmole/liter), $NaHCO_3$ (6.65 mmole/liter), NaH_2PO_4 (2.96 mmole/liter), Na_2HPO_4 (0.15 mmole/liter), glucose (12.8 mmole/liter), and 7.36% of GIB No. 133 tissue culture medium (Grand Island Biological, Grand Island, New York), a complex medium containing 10% fetal calf serum, plus salt ions, vitamins, and free amino acids. Inclusion of this medium, specifically prepared for this laboratory to contain no K^+ ion except for that in the calf serum, prolongs the survival time of frog muscle cells if bacterial and fungal contaminations are avoided.

To each 10 ml of the above experimental solution, we added: 0.1 ml (10 mg/ml) of penicillin G (sodium) (Upjohn, Lot PF171), 0.1 ml (10 mg/ml) of streptomycin sulfate (Pfizer, Lot 04357), 0.05 ml of insulin (80 units/ml) (Iletin, Eli Lilly), and 0.05 to 0.1 ml of radioactive isotope solution (see below). K^{42}, Rb^{86}, Cs^{134} were obtained from Oak Ridge National Laboratories, Oak Ridge, Tenn., in the form of chlorides dissolved in 1 N HCl. Carrier-free Na^{22} in the form of NaCl in 0.5 N HCl was obtained from Nuclear Science and Engineering Corp., Pittsburgh, Pa. The isotopic solutions were neutralized with NaOH, and the Na^+ introduced was taken into account when the experiment was of such a nature that the added Na^+ ion be-

Downloaded from jgp.rupress.org on December 16, 2012

Published March 1, 1966

came significant. The neutralized solution of K^{42} usually contained about 4 to 6 mc/ml of the isotope; Rb^{86}, about 9 to 12 mc/ml; Cs^{134}, about 2 mc/ml; and Na^{22}, about 0.1 mc/ml. Neutralized K^{42} solutions were added directly to the experimental tubes without further dilution. Rb^{86} and Cs^{134} were diluted about one to ten before

TABLE I

COMPOSITION OF MODIFIED RINGER'S SOLUTIONS

(For other components present, see text.)

part i				*part ii*			
Solution No.	NaCl (0.118 M)	$(p_i^+)_{ex}$ K*Ac (0.118 M)	$(p_j^+)_{ex}$ KAc (0.118 M)	Solution No.	NaCl (0.118 M)	Cs‡Ac (0.118 M)	KAc (0.118 M)
A_1	99.0	1.0	0	A_1	77.5	2.5	0
A_2	97.5	2.5	0	A_2	75.0	5.0	0
A_3	95.0	5.0	0	A_3	70.0	10.0	0
A_4	90.0	10.0	0	A_4	55.0	25.0	0
A_5	75.0	25.0	0				
A_6	50.0	50.0	0	B_1	57.5	2.5	20
				B_2	55.0	5.0	20
				B_3	50.0	10.0	20
B_1	79.0	1.0	20	B_4	35.0	25.0	20
B_2	77.5	2.5	20	B_5	10.0	50.0	20
B_3	75.0	5.0	20				
B_4	70.0	10.0	20	C_1	27.5	2.5	50
B_5	55.0	25.0	20	C_2	25.0	5.0	50
B_6	30.0	50.0	20	C_3	20.0	10.0	50
B_7	20.0	60.0	20	C_4	5.0	25.0	50
B_8	0.0	80.0	20				
B_9	0.0	100.0	20				
C_1	49.0	1.0	50				
C_2	47.5	2.5	50				
C_3	45.0	5.0	50				
C_4	40.0	10.0	50				
C_5	25.0	25.0	50				
C_6	0.0	50.0	50				
C_7	0.0	60.0	50				
C_8	0.0	80.0	50				
C_9	0.0	100.0	50				

* K^{42}-tagged KAc solution.

‡ Cs^{134}-tagged CsAc solution.

addition. Because of the short half-life, a high specific activity of the K^{42} is essential. A high activity of Rb^{86} is also necessary because the counting efficiency for this isotope is low (6.4%). (We also found that the volume of the water in the Rb^{86} sample has a significant effect on its counting efficiency.)

All nonradioactive chemicals were of cp grade (largely Merck Reagent or Baker Analyzed). Rubidium and cesium salts were obtained from Penn Rare Metals, Inc., Revere, Pa. (purity 99% in some cases and 99.9% in others).

Downloaded from jgp.rupress.org on December 16, 2012

Published March 1, 1966

RESULTS

Time to Reach New Equilibrium Ionic Levels

When frog sartorius muscles are incubated in a modified Ringer solution containing 50 mmole/liter of K^{42}-labeled K^+ ion, the concentration of intracellular labeled K^+ ion rises to reach a new equilibrium after 10 to 20 hr (24°C)[3] (solid circles in Fig. 6). This finding is in general accord with earlier

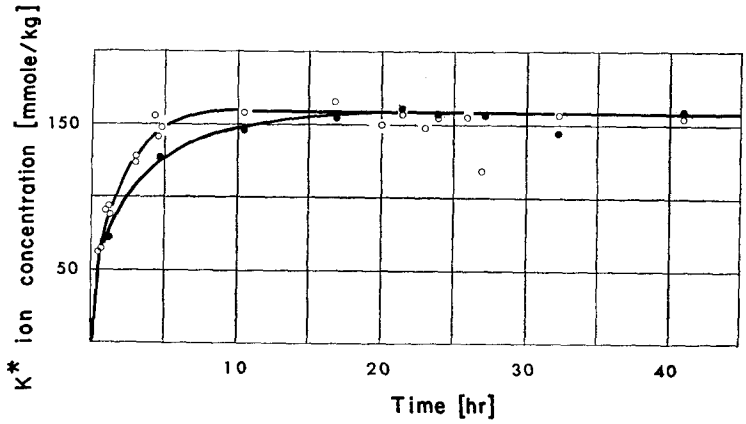

FIGURE 6. Time course of labeled K^+ ion uptake by frog sartorius muscles (24°C). Sartorius muscles were placed in Ringer–GIB–serum solution containing 50 mmole/liter (solid circles) and 100 mmole/liter (open circles) of K^{42}-labeled K acetate (four muscles per solution). Muscles were removed (two at a time) at intervals, weighed, and their radioactivity assayed directly before replacing them in the solution to further equilibrate. Considerable variation in the weights of the tissues was observed in this and other similar time courses.

observations of Fenn and Cobb (13), Conway (14), and Harris (15). Since neither Fenn and Cobb nor Conway employed radioactive tracer, this close correspondence of the data indicates that, at the intensity employed, the radioactivity produces no significant alterations of the muscle cells within the length of time investigated. We reached the same conclusion from permeability studies (16).

The open circles in Fig. 6 represent experimental results for muscles bathed in 100 mmole/liter of labeled K^+ ion; the data indicate that the time course is somewhat faster than at the lower concentration of 50 mmole/liter. However, a difference between the equilibrium concentrations of labeled K^+ ion in the two cases is not discernible.

[3] It is unfortunate that a great deal of the pioneering work on K^+ ion distribution reported by Fenn and his coworkers (13) and by Steinbach (17) was based on a soaking time of 5 hr (at room temperature). On the basis of the present data, this is not long enough to insure the attainment of the new equilibrium ionic levels.

Downloaded from jgp.rupress.org on December 16, 2012

Published March 1, 1966

For Rb^+ at 100 mmole/liter external concentration, it took 25 hr to reach the new equilibrium (Fig. 7). A somewhat greater scattering of the data is evident when plotted on the basis of initial weight. For this reason, all subsequent data are presented on the basis of final weights.

For Cs^+ ion at 25 mmole/liter external concentration, the new equilibrium is reached in about 22 hr (Fig. 8). The study of Cs^+ ion at high concentrations is prohibited by the tendency of Cs^+ ion at high concentrations to form crystals with magnesium and phosphate in a medium of neutral or higher pH. Ringer's

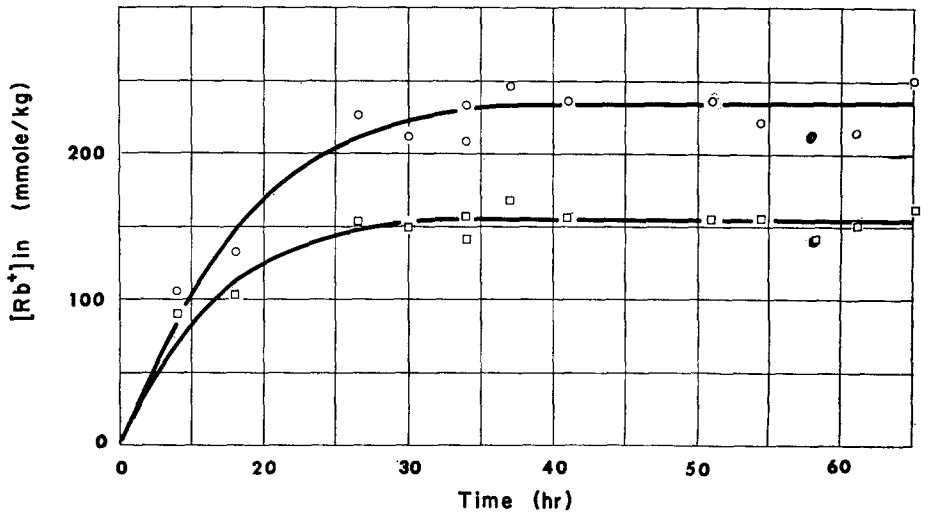

FIGURE 7. Time course of labeled Rb^+ ion uptake by frog sartorius muscles (25°C). Technique as used in Fig. 6 except six muscles placed in Ringer–GIB–serum solution containing 100 mmole/liter of Rb^{86}-labeled Rb acetate. The initial external K^+ ion concentration was 0.1 to 0.2 mmole/liter. The data are plotted on the basis of both final (squares) and initial (circles) weights of the tissues.

solution, designed to preserve the muscle for a lengthy period of time, must contain Mg^{++} and phosphate ions at near neutral pH.

Fig. 9 shows the time course of equilibrium for labeled Na^+ ion at 25°C. Equilibrium was reached in some 30 hr at this temperature.

As a rule, for all ions studied, once a new equilibrium is reached, this level remains steady for many hours.

The Nature of Competition in Ionic Accumulation

Fig. 10 illustrates the dependence of the equilibrium intracellular Cs^+ ion concentration on the external K^+ ion concentration. Thus, at 25 mmole/liter external Cs^+ ion concentration and 2.5 mmole/liter of K^+ ion, the equilibrium concentration of Cs^+ ion in the cell is about 80 mmole/kg (see Fig. 8). In the presence of 50 mmole/liter of K^+ ion, the Cs^+ ion concentration in muscle

Downloaded from jgp.rupress.org on December 16, 2012

Published March 1, 1966

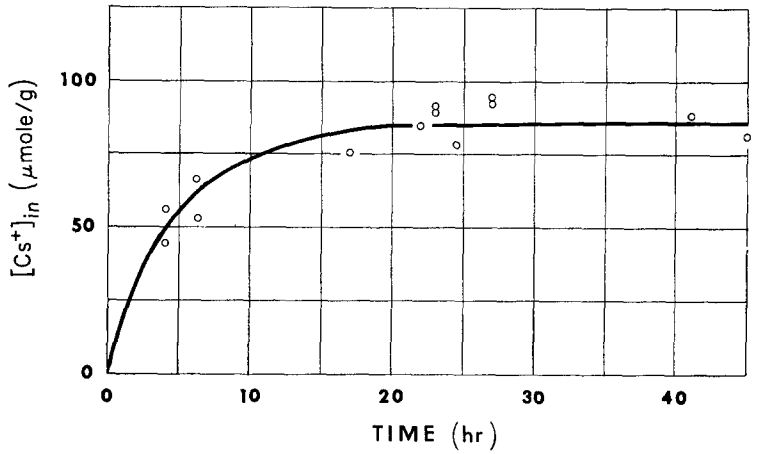

FIGURE 8. Time course of labeled Cs^+ ion uptake by frog sartorius muscles (24°C). Technique as in Fig. 6 except four sartorius muscles placed in a Ringer–GIB–serum solution (pH 7.0) containing 25 mmole/liter of Cs^{134}-labeled Cs acetate. The initial external K^+ ion concentration was 0.1 to 0.2 mmole/liter. Internal Cs^+ ion concentration calculated on the basis of the final tissue weight.

cells reaches a level only a little above 40 mmole/kg. If, after the Cs^+ ion level reaches equilibrium in the presence of 2.5 mmole/liter K^+ ion, the muscle is transferred to a solution containing 50 mmole/liter K^+ ion, the intracellular Cs^+ ion concentration falls to the same level as in the muscle which had been

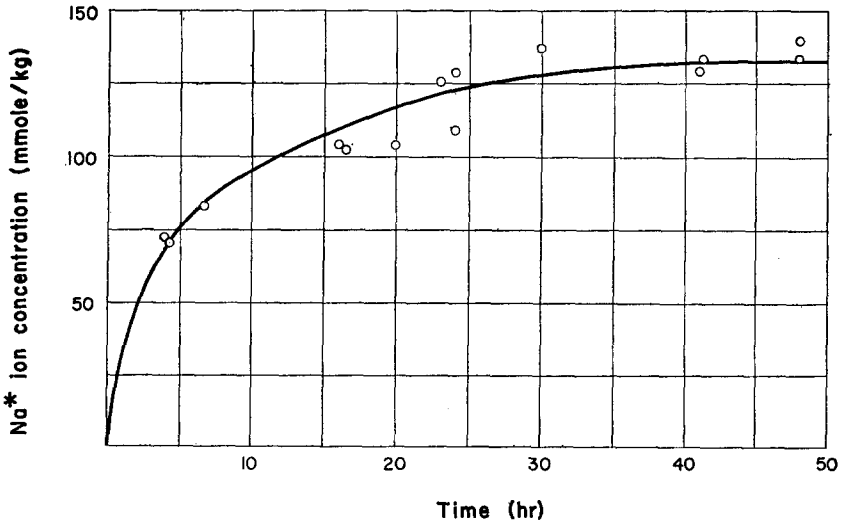

FIGURE 9. Time course of labeled Na^+ ion uptake by frog sartorius muscles in a Ringer solution with a low K^+ ion and high Na^+ ion concentration (25°C). Technique as in Fig. 6 except six sartorius muscles were placed in a Ringer–GIB–serum solution containing 0.5 mmole/liter KCl and 170.5 mmoles/liter of Na in the form of acetate and phosphates.

Downloaded from jgp.rupress.org on December 16, 2012

Published March 1, 1966

in the presence of 50 mmole/liter of K^+ ion throughout. This observation demonstrates that an increase of external K^+ ion concentration reduces the rate of entry of Cs^+ ion into the cell and the equilibrium level of Cs^+ ion in the cell.

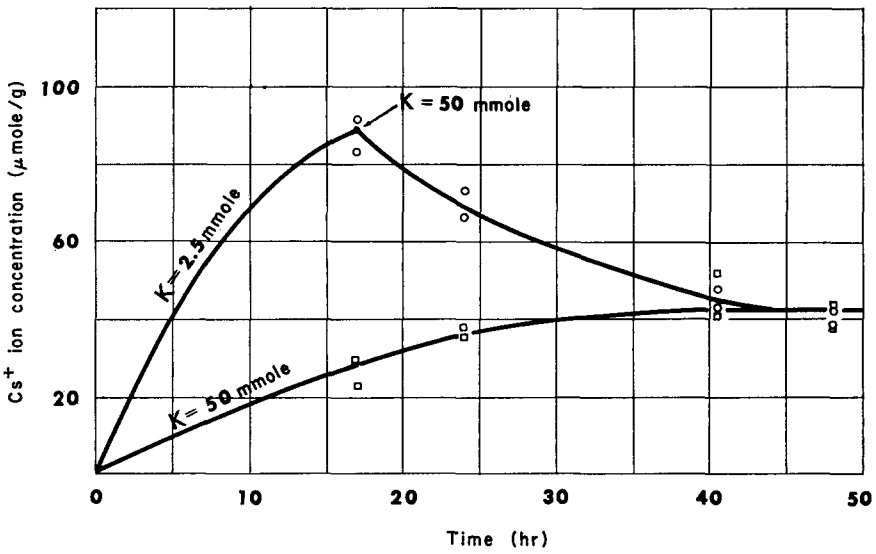

FIGURE 10. Effect of K^+ ion on level of labeled Cs^+ ion accumulation. Frog sartorius muscles incubated in Ringer's solution containing 25 mmole/liter labeled Cs^+ ion and 2.5 mmole/liter K^+ ion (24°C); their pairs incubated in Ringer's solution containing the same amount of labeled Cs^+ ion and 50 mmole/liter of K^+ as acetate (squares). The weights and radioactivity of the muscles were determined after 17 hr and the muscles in the solution containing 2.5 mmole/liter K^+ ion transferred to another Ringer's solution containing 50 mmole/liter K^+ (circles). The weight and radioactivity of these muscles, as well as those which had been in the Ringer solution with 50 mmole/liter K^+ ion were then assayed at intervals.

K^+ Ion Accumulation and Competition

Fig. 11 shows reciprocal plots of the equilibrium concentrations of K^{42}-labeled K^+ ion, in the presence of varying amounts of nonlabeled K^+ ion as competing ion (0, 20, and 50 mmole/liter). These data demonstrate competition in K^+ ion accumulation in the muscle cells. The intercepts in $(\text{mole/liter})^{-1}$ are: 7.321×10^{-3} with no competing ion; 7.14×10^{-3} with 20 mmole/liter of competing nonlabeled K^+ ion; 6.49×10^{-3} with 50 mmole/liter of competing nonlabeled ion.

Na^+ Ion Accumulation and Competition

Fig. 12 shows reciprocal plots of the equilibrium labeled Na^+ ion concentration in the presence of 0.5 mmole/liter and 10 mmole/liter competing K^+ ion.

Downloaded from jgp.rupress.org on December 16, 2012

Published March 1, 1966

Rb^+ Ion Accumulation and Competition

Fig. 13 presents analogous studies on the equilibrium distribution of labeled Rb^+ ion. The intercepts in $(mole/liter)^{-1}$ are: 8.11×10^{-3} with no competing ion present; 9.8×10^{-3} with 20 mmole/liter of competing nonlabeled Rb^+ ion; and 10.2×10^{-3} with 50 mmole/liter of competing nonlabeled Rb^+ ion.

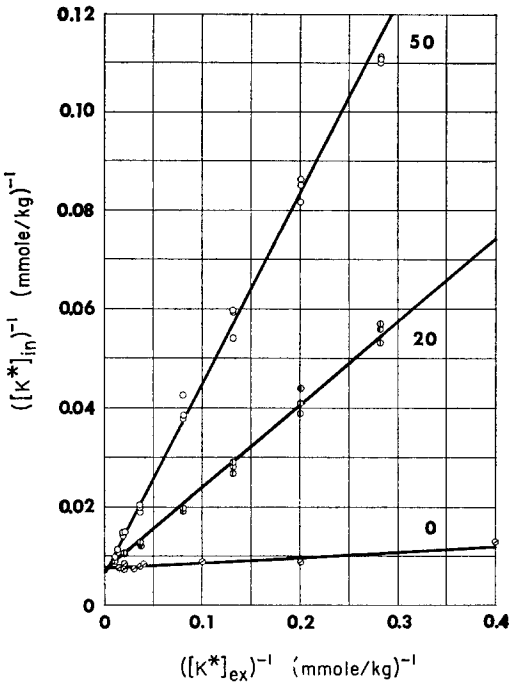

FIGURE 11. Intracellular labeled K^+ ion concentration plotted reciprocally against the external labeled K^+ ion concentration, with which it is in equilibrium, in the presence of 0, 20, and 50 mmole/liter of nonlabeled K acetate. Labeled K^+ was also in the form of acetate salt. Each point represents the labeled K^+ ion concentration in a single frog sartorius muscle; lines obtained by the method of least squares. On the lowest curve within the area from $([K^+]_{ex})^{-1} = 0$ to 0.05 $(mmole/liter)^{-1}$ and from $([K^+]_{in})^{-1} = 0$ to 0.01 $(mmole/kg)^{-1}$, a total of 23 points was determined; they fall so close to one another that only a few could be represented. All the others would be superimposed on these. Data from two series of experiments (13 June 1963; 17 September 1963).

Cs^+ Ion Accumulation and Competition

Fig. 14 shows reciprocal plots of the effect of varying the external K^+ ion concentration on the equilibrium concentration of Cs^+ ion (solid lines). The intercepts in $(mole/liter)^{-1}$ are: 10.6×10^{-3} with no competing ion present; 12.5×10^{-3} with 20 mmole/liter of competing K^+ ion; 24.0×10^{-3} with 50

Downloaded from jgp.rupress.org on December 16, 2012

Published March 1, 1966

mmole/liter of competing K^+ ion present. The two dotted lines were taken from Fig. 11 to show by contrast the much smaller effect the same concentrations of nonlabeled K^+ ion exercised on the equilibrium concentration of labeled K^+ ion.

DISCUSSION AND CONCLUSION

The major results presented in this communication consist of four sets of equilibrium ionic distribution data. Two of these show the effect of nonlabeled

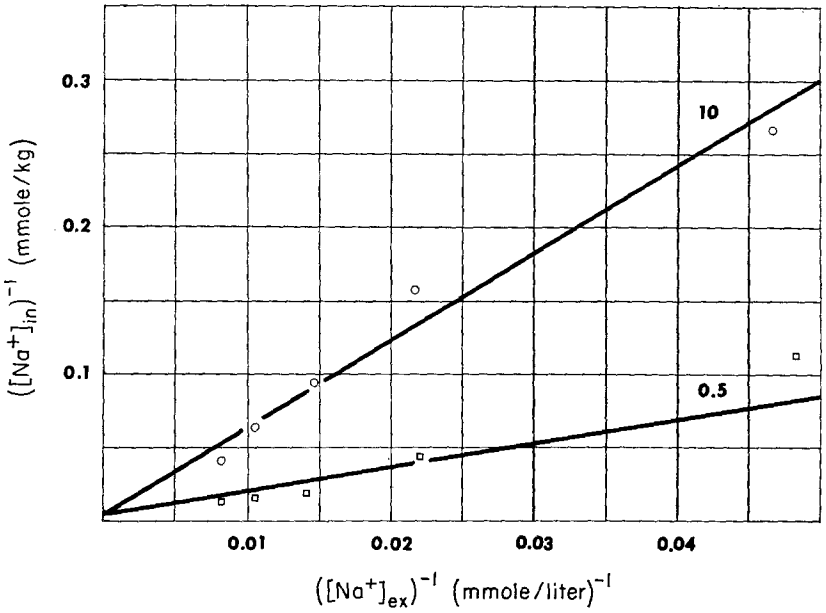

FIGURE 12. Equilibrium intracellular Na^+ ion concentration plotted reciprocally against the extracellular Na^+ ion concentration, in the presence of 0.5 and 10 mmole/liter of K^+ ion. Time of equilibration was 25 hr (at 25°C). Na^+ ion concentration assayed by flame photometry (for details of procedure, see reference 3, p. 201). Each point represents the value from three muscles; lines drawn by visual inspection.

alkali metal ion on the equilibrium distribution of labeled alkali metal ion of the same chemical species (i.e., K^+ ion on K^{42}-labeled K^+ ion (Fig. 11), and Rb^+ ion on Rb^{86}-labeled Rb^+ ion (Fig. 13)). The other two series show the effect of one nonlabeled alkali metal ion (i.e., K^+ ion) on the equilibrium distribution of two chemically different alkali metal ions (i.e., Na^{22}-labeled Na^+ ion (Fig. 12), and Cs^{134}-labeled Cs^+ ion (Fig. 14)).

Within the lower concentration range, the data of the first two sets of experiments (Figs. 11 and 13) are in essential agreement with both the Donnan membrane model and with the model arising from the association-induction hypothesis; we have mentioned this formal analogy earlier in discussing Equations 5 and 16. A comparison of both Figs. 11 and 13 with Fig. 2 also

Downloaded from jgp.rupress.org on December 16, 2012

Published March 1, 1966

shows that there is a fair degree of quantitative accord between the experimental data and the two theoretical models.

In the other two sets of experiments we studied the competing effect of a chemically different species. The result shown in Fig. 14, for example, shows that the same concentration of K^+ ion produces about three times as effective competition against Cs^+ ion as against K^+ ion. K^+ ion is even more effective

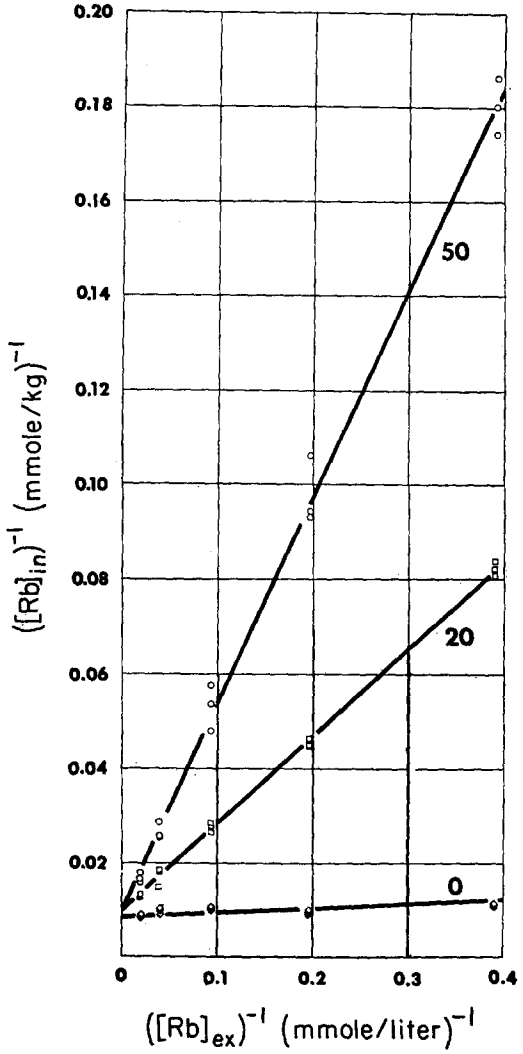

FIGURE 13. Intracellular labeled Rb^+ ion concentration plotted reciprocally against the external Rb^+ ion concentration with which it is in equilibrium (26°C). Competing nonlabeled Rb^+ ion concentrations were 0, 20, and 50 mmole/liter respectively. Labeled Rb^+ ion was in the form of acetate. Each point represents the labeled Rb^+ ion concentration in a single frog sartorius muscle; lines obtained by the method of least squares.

Downloaded from jgp.rupress.org on December 16, 2012

Published March 1, 1966

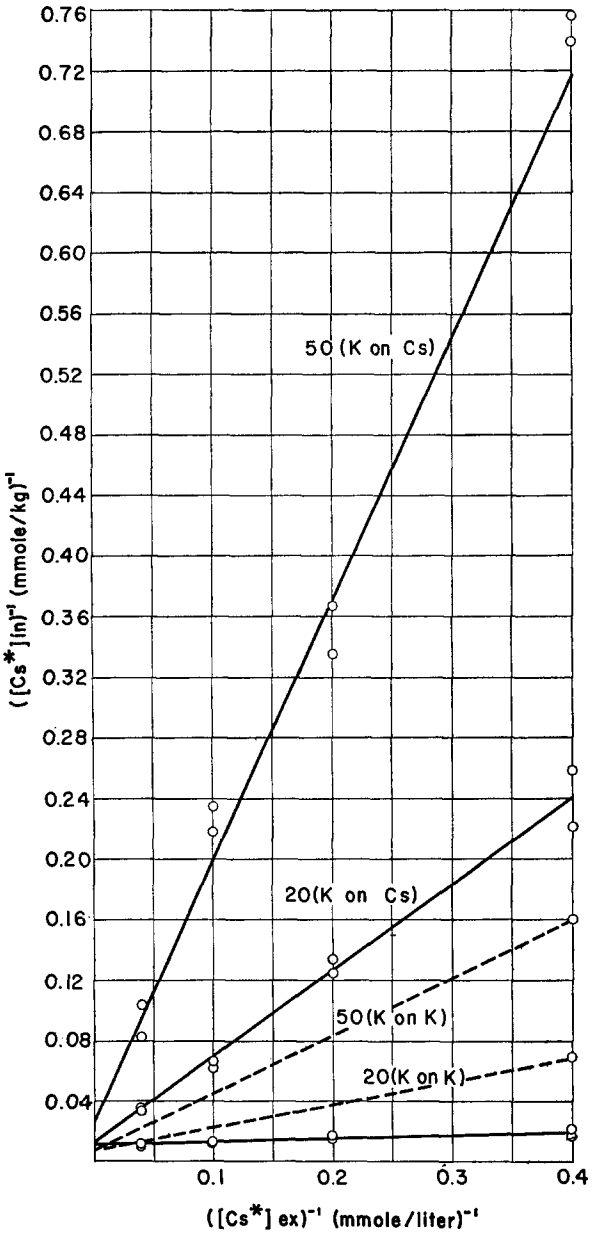

FIGURE 14. Equilibrium labeled Cs^+ ion concentration in muscle cells plotted reciprocally against the external Cs^+ ion concentration with which it is in equilibrium. Competing K^+ ion concentrations are 0, 20, and 50 mmole/liter respectively. Both Cs^+ and K^+ were in the form of acetates (24°C). Each point represents a single determination on one frog sartorius muscle; lines obtained by the method of least squares. The effect of K^+ ion on the accumulation of labeled K^+ ion (dotted lines) taken from Fig. 12 for comparison.

Downloaded from jgp.rupress.org on December 16, 2012

Published March 1, 1966

in competing against Na^+ ion accumulation (Fig. 12). As stated previously, within the limits of our experimental error, the Donnan theory predicts no difference between the competitive effects of different ions. *From this we conclude that the results of the present investigation do not support the concept that the ions studied accumulate in cells according to the Donnan membrane equilibrium; they are, however, consistent with the model according to the association-induction hypothesis.*

Let us now analyze the experimental data quantitatively according to the latter model. The experimentally measured intercepts from K^+ ion accumulation studies correspond respectively to 137, 140, and 154 mmole of anionic adsorption sites per kg final weight. Ignoring competing ions other than K^+ ion (e.g., Na^+), the mean apparent free energies of association are -3.74, -3.74, and -3.81 kcal/mole respectively. On the other hand, combining the equations corresponding to the lower curve of Fig. 12 and the lowest curve of Fig. 11, one can solve the equations simultaneously to obtain the apparent association constants for both Na^+ and K^+ ions (in this case taking into account Na^+ ion competition). The value for Na^+ ion is then 0.996 and for K^+ ion is 633 $(\text{mole/liter})^{-1}$. On the basis of these values, one can calculate, from the upper two curves of Fig. 11, additional values of the apparent association constant for K^+ ion, namely, 648 and 720 $(\text{mole/liter})^{-1}$. The average of all these values is 665 $(\text{mole/liter})^{-1}$. The corresponding apparent standard-free energy of association is 0 for Na^+ ion; -3.82, -3.84, and -3.89 kcal/mole for K^+ ion.[4] Fig. 15 presents the data given in Fig. 11 in a linear plot. The curves are theoretical curves, calculated from Equation 10 on the basis of the following: (*a*) a single type of adsorption site, for which the association constant of K^+ ion is the average obtained from the reciprocal plot, i.e. 665 $(\text{mole/liter})^{-1}$, and where the apparent association constant for Na^+ ion is 0.996; (*b*) $[K^+]_{ins}$ was ignored.

The total concentration of the adsorption site, $[f^-]^{total}$, 140 mmole/kg, is obtained by curve fitting. Since the linear plot as a rule better displays the data of the high concentration range, whereas the reciprocal plot emphasizes the lower concentration range, one may anticipate that the $[f^-]^{total}$ obtained from this linear plot is more reliable. In the present case, however, the value 140 mmole/kg is close to 137 mmole/kg, obtained from the reciprocal plot at zero-inhibiting ion concentration. In discussing the data of Fig. 5, we mentioned that the curve with inhibiting-ion concentration at zero yields the best estimate of the total number of sites among the various reciprocal curves.

[4] The inclusion of the Na^+ ion data is a compromise. In order to demonstrate significant K^+ ion competition for sites adsorbing Na^+ ion, we had to reduce the K^+ ion concentration to 0.5 mmole/liter (from a normal serum value of 2.5 mmoles/liter) (Fig. 12). In this concentration range there is cooperative interaction between K^+ and Na^+ ion and, therefore, the general equation (to be presented elsewhere), rather than special Equation 10, applies. Reserving this important subject for a later paper (18), we have applied Equation 10 as a first approximation. We estimate that the error thus introduced is much smaller than that which would result from ignoring Na^+ ion altogether.

Downloaded from jgp.rupress.org on December 16, 2012

Published March 1, 1966

Similarly, the data of Fig. 13 yield 123, 102, and 98.5 mmole of adsorption sites for Rb^+ ion per kg of final weight of the cells. If one accepts a $\tilde{K}^{\infty \to T}_{Na(Ac)}$ value of 0.996, the three curves give mean apparent association constants for Rb^+ ion of 840, 735, and 704 $(mole/liter)^{-1}$ respectively (average = 755), with corresponding mean apparent standard-free energies of adsorption equal to −3.93, −3.91, and −3.88 kcal/mole (average = −3.92 kcal/mole). In

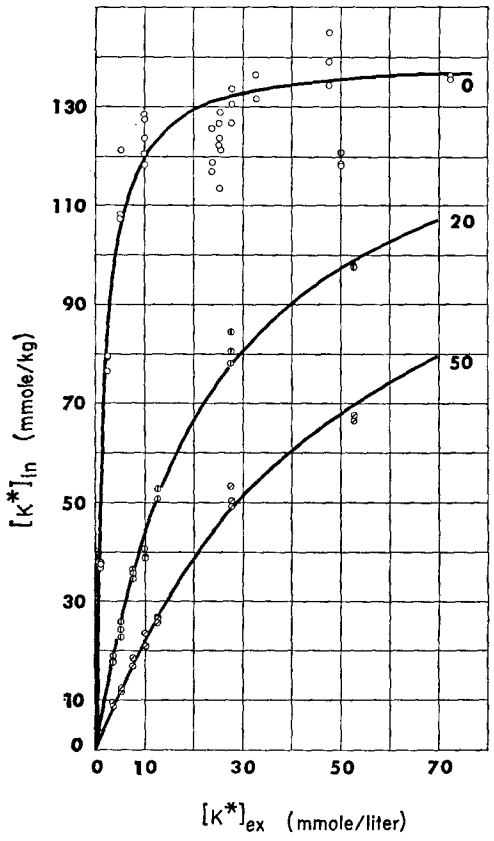

FIGURE 15. Equilibrium intracellular labeled K^+ ion concentration at various external K^+ ion concentrations (24°C). Data are the same as in Fig. 11. Curves theoretically calculated on the basis of Equation 10 and the following: (*a*) $q^{\infty \to ins}_{ik} = 0$; (*b*) one type of adsorption site at a concentration of 140 mmole/kg; and (*c*) an association constant of 6.65×10^{-2} for K^+ ion and 0.996 for Na^+ ion in M^{-1}.

Fig. 16, the experimental data from Fig. 13 are plotted linearly. The curves were again calculated theoretically, using the average value of $\tilde{K}^{\infty \to T}_{Rb(Ac)} = 755$ $(mole/liter)^{-1}$, and a total of 115 mmole of adsorption sites per kg of final weight.

In the same way, the data of Fig. 14 yielded the number of total adsorption sites for Cs^+ ion as: 94.3 mmole/kg ($[K]_{ex} = 0$), 80.0 mmole/kg ($[K]_{ex} = 20$ mmole/liter), and 41.7 mmole/kg ($[K]_{ex} = 50$ mmole/liter). There is, thus, a sharply decreasing value of the fixed anion concentration with higher competing K^+ ion concentrations. The single value of the mean apparent association constant for Cs^+ ion obtained is 488 $(mole/liter)^{-1}$; the corresponding

Downloaded from jgp.rupress.org on December 16, 2012

Published March 1, 1966

mean apparent free energy of association is −3.66 kcal/mole. The association constants for K^+ ion obtained from this set of data are 1060 and 703 (mole/liter)$^{-1}$, and their corresponding mean apparent free energies of association are −4.11 and −3.87 kcal/mole respectively.

Thus, in general, each ion has a specific association constant, $\tilde{K}_{i(k)}^{\infty \to T}$, and exercises a specific and different competitive effect on the adsorption of another ion. These competitive effects are quantitatively far beyond the limit of specificity offered by the Donnan model on the basis of differences of ac-

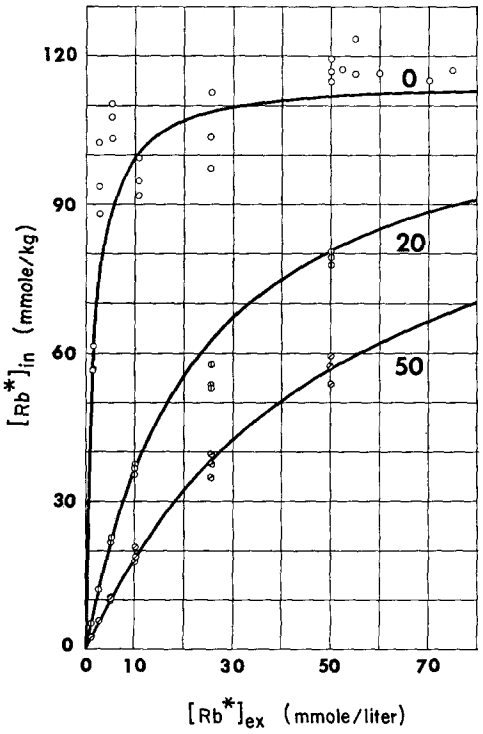

FIGURE 16. Equilibrium labeled Rb^+ ion concentration in muscle cells at various extracellular Rb^+ ion concentrations (26°C). Points are the same as those in Fig. 13. We calculated curves theoretically on the basis of Equation 10 and the following: (*a*) $q_{i(k)}^{\infty \to ins} = 0$; (*b*) one type of adsorption site at a concentration of 115 mmole/kg of final fresh weight; and (*c*) $\tilde{K}_{Rb(Ac)}^{\infty \to T} = 755\ M^{-1}$.

tivity coefficients (less than 2%) and qualitatively follow a rank order of effectiveness ($Rb^+ > K^+ > Cs^+ > Na^+$) entirely different from that anticipated on the basis of activity coefficients ($Na^+ > K^+ > Rb^+ > Cs^+$), but are the same rank order as that which Cohen found for ion accumulation in living as well as dead *Chlorella* cells ($Rb^+ > K^+ > Cs^+ > Na^+$) (reference 19; see also reference 20). (For further discussion on the significance of these rank orders in alkali metal ion adsorption, see Ling (3) and Eisenman (21).)

The experimental data support the association-induction hypothesis in still another way. Fig. 7 shows that in terms of the *initial* fresh weight, a total as high as 240 mmole/kg of fixed anionic sites is present in the frog sartorius muscle; other data (in Figs. 12 and 13) gave somewhat lower values. According

Downloaded from jgp.rupress.org on December 16, 2012

Published March 1, 1966

to the association-induction hypothesis, the majority of these sites belong to the β- and γ-carboxyl groups of the cell proteins. One must now determine whether this theoretical expectation is supported by the body of rather accurate analytical data on the composition of muscle proteins.

Leaving the details to the Appendix, calculation from the best available data yields a total of 260 to 288 mmole of free anionic sites per kg of fresh muscle cells on the proteins known to be present in muscle cells. These figures do not include the small amounts of nucleic acids and phospholipids as well as the larger amounts of creatinephosphate (21.8 mmole/kg) and ATP (5 mmole/kg) in the muscle cells (see reference 3, Table 9.2). Complexed or adsorbed on cationic sites, these compounds add a significant amount of secondarily fixed anions as potential adsorption sites to the 260 to 288 mmole/kg of proteinaceous fixed anions. Elsewhere, we have presented evidence that salt linkages are important in maintaining the structure of the living cell (reference 3, sect. 9.4). Since, by and large, the structure of the cell is preserved (though swollen), even in the highest salt concentration studied, there must be a sufficient number of fixed anions engaged in these salt linkages. Thus, it appears that the number of fixed anionic sites corresponds well with those calculated from the present series of experiments. Since no other component in the living muscle cell contains anionic sites at this concentration, *this agreement is consistent with the concept that it is the free β-carboxyl group of aspartic acid residues and the free γ-carboxyl group of glutamine acid residues on the cellular proteins which selectively adsorb most of the alkali metal ions.*

Appendix

The Concentration of Fixed Anionic Sites in Muscle Cells

Available data indicate that the protein concentration of muscle tissue falls between 18.5 and 25%. Since there is evidence that frog muscle contains somewhat more water than mammalian tissue, we shall choose 18% as a lower limit of protein concentration and 20% as the higher limit. The average amino acid residue weight of muscle protein is equal to 111 (see reference 3, p. 48). Dividing this into the total protein concentration, one obtains 1.63 and 1.80 mole/kg of amino acid residues in proteins, respectively.

The latest data of Lowey and Cohen (22) show that rabbit myosin contains 17.4% of free anionic residues. (This value agrees reasonably well with Mihalyi's titration data which correspond to 18% (23).) If one assumes that the upper limit of myosin content in muscle proteins is 57% (24), that of actin is 15% (25), and that of tropomyosin is 2.6% (26), the remainder would constitute 25.4% of the total muscle proteins. This remainder contains: aldolase, triosephosphate dehydrogenase, glycogen phosphorylase, ATP-creatine transphosphorylase, and myokinase. Actin contains 13.8% free anionic side chains (27); tropomyosin (frog), 28.3% (28); aldolase, 9.3% (29); triosephophate dehydrogenase, 6.5% (30); phosphorylase (rabbit), 13.5% (30); myokinase, 13.5% (31); and ATP-creatine transphosphorylase, 22.8% (32).

Downloaded from jgp.rupress.org on December 16, 2012

Published March 1, 1966

The average free anionic group of the last five enzymes amounts to 13.1%. If one assumes that the 25.4% of muscle proteins not accounted for by myosin, actin, or tropomyosin has this concentration of the free anionic groups, then the average percentage of anionic residues in muscle proteins would be: $0.57 \times 0.174 + 0.15 \times 0.138 + 0.026 \times 0.238 + 0.254 \times 0.131 = 16\%$. By multiplying this value into the lower limit of amino acid residue concentration in the cell (1.63 mole/kg), one obtains 260 mmole/kg of fresh weight of fixed anionic sites. Using the higher protein concentration (1.81 mole/kg), one obtains 288 mmole/kg.

We thank Drs. Frank Elliott, George Karreman, and Margaret Neville for their critical reading of the manuscript.

This investigation was supported in part by the National Institutes of Health Research Grant GM-11422-01, and by a research grant from the National Science Foundation (GB-13). The investigator was also supported by a Public Health Service Research Development Fund (GM K3-19032).

Received for publication 16 February 1965.

REFERENCES

1. BAIRD, S. L., KARREMAN, G., MUELLER, H., and SZENT-GYÖRGYI, A., *Proc. Nat. Acad. Sc.*, 1957, **43**, 705.

BOYLE, P. J., and CONWAY, E. J., *J. Physiol.*, 1941, **100**, 1.

ERNST, E., and MOROCZ, E., *Enzymologia*, 1940–41, **9**, 127.

FENN, W. O., *Physiol. Rev.*, 1936, **16**, 450; 1940, **20**, 377.

FISCHER, M. H., and MOORE, G., *Am. J. Physiol.*, 1908, **20**, 330.

JOSEPH, N. R., ENGEL, M. B., and CATCHPOLE, H. R., *Nature*, 1961, **191**, 1175.

KATZ, J. A., *Arch. ges. Physiol.*, 1896, **63**, 1.

LUBIN, M., and SCHNEIDER, P. B., *J. Physiol.*, 1957, **138**, 140.

MENOZZI, P., NORMAN, D., POLLERI, A., LESTER, G., and HECHTER, O., *Proc. Nat. Acad. Sc.* 1959, **45**, 80.

NASONOV, D. N., Local Reaction of Protoplasm and Gradual Excitation, (in English), Israel Program for Scientific Translation, Jerusalem, 1962, (available from Office of Technical Service, U. S. Dept. of Commerce, Washington, D. C.).

NEUSCHLOSS, S. M., *Arch. ges. Physiol.*, 1924, **204**, 374.

RELMAN, A. S., LAMBIE, A. T., BURROW, B. A., and RAY, A. M., *J. Clin. Inv.*, 1957, **36**, 1249.

SHAW, F. H., and SIMON, S. E., *Australian J. Exp. Biol. and Med. Sc.*, 1955, **33**, 153.

SHAW, F. H., SIMON, S. E., and JOHNSTONE, B. M., *J. Gen. Physiol.*, 1956, **40**, 1.

STEINBACH, H. B., *Cold Spring Harbor Symp. Quant. Biol.*, 1940, **8**, 241.

TROSCHIN, A. S., Das Problem der Zellenpermeabilitaet, Cristar Fischer, Jena, 1958 (for English translation of an important part of this thesis, see the Nasonov reference above).

2. LING, G. N., *Am. J. Physiol.*, 1951, **167**, 806.

LING, G. N., *in* Symposium on Phosphorus Metabolism, (W. D. MCELROY and G. GLASS, editors), Baltimore, The Johns Hopkins Press, 1952, **2**, 748.

Downloaded from jgp.rupress.org on December 16, 2012

Published March 1, 1966

3. LING, G. N., A Physical Theory of the Living State: The Association-Induction Hypothesis, Blaisdell Publishing Co., New York, 1962.
4. LING, G. N., *Fed. Proc.*, 1965, **24**, S103.
5. DONNAN, F. G., *Z. Elektrochem.*, 1911, **17**, 572.
6. BOLAN, T. R., The Donnan Equilibrium, London, G. Bell & Sons, 1932.
7. HODGMAN, C. D., WEAST, R. C., and SELBY, S. M., Handbook of Chemistry and Physics, Cleveland, The Chemical Rubber Publishing Co., 42nd edition, 1960–61, 2611.
8. LING, G. N., *Perspectives Biol. and Med.*, 1965, **9**, 87.
9. LING, G. N., *Texas Rep. Biol. Med.*, 1964, **22**, 244.
10. LING, G. N., *Biopolymer Symp.*, 1964, **1**, 91.
11. LING, G. N., The Physical State of Water in the Living Cells and Model Systems, *Ann. New York Acad. Sc.*, 1965, **125**, 401.
12. LING, G. N., *in* Discussion of Symposium on Membrane Transport and Metabolism, Czechoslovak Academy of Sciences, New York Academic Press, Inc., 1960, 314.
13. FENN, W. O., and COBB, D. M., *J. Gen. Physiol.*, 1934, **17**, 629. FENN, W. O., COBB, D. M., HEBENAUER, A. H., and MARSH, B. S., *Am. J. Physiol.*, 1934, **110**, 74.
14. CONWAY, E. J., *Nature*, 1946, **157**, 715.
15. HARRIS, E. J., *J. Physiol.*, 1952, **117**, 278.
16. LING, G. N., and OCHSENFELD, M. M., *Biophysic. J.*, 1965, **5**, 777.
17. STEINBACH, H. B., *J. Cell. and Comp. Physiol.*, 1937, **9**, 429.
18. LING, G. N., *Fed. Proc., Symp. Biophysic. Physic. Chem. on Connective Tissue*, in press.
19. COHEN, D., *J. Gen. Physiol.*, 1962, **45**, 959.
20. EISENMAN, G., *Bol. Inst. Estud. Méd. Biol. Mexico*, 1963, **21**, 155.
21. EISENMAN, G., *Biophysic. J.*, 1962, **2**, 259.
22. LOWEY, S., and COHEN, C., *J. Mol. Biol.*, 1962, **4**, 293.
23. MIHALYI, E., *Enzymologia*, 1950, **14**, 224.
24. BATE-SMITH, E. C., *Proc. Roy. Soc. London, Series B*, 1937, **124**, 136.
25. HASSELBACH, W., and SCHNEIDER, G., *Biochem. Z.*, 1951, **321**, 462.
26. BAILEY, K., *Symp. Soc. Expt. Biol.*, 1955, **9**, 183.
27. KOMINZ, D. R., HOUGH, A., SYMONDS, P., and LAKI, K., *Arch. Biochem. and Biophysics*, 1954, **50**, 148.
28. SAAD, F., KOMINZ, D. R., and LAKI, K., *J. Biol. Chem.*, 1959, **234**, 551.
29. VELICK, S. F., and RONZONI, E., *J. Biol. Chem.*, 1948, **173**, 627.
30. APPELMAN, M. M., YUNIS, A. R., KREBS, E. G., and FISCHER, E. H., *J. Biol. Chem.*, 1963, **238**, 1358.
31. MAHOWALD, T. A., NOLTMAN, E. A., and KUBY, S. A., *J. Biol. Chem.*, 1962, **237**, 1138.
32. NOLTMAN, E. A., MAHOWALD, T. A., and KUBY, S. A., *J. Biol. Chem.*, 1962, **237**, 1146.

Downloaded from jgp.rupress.org on December 16, 2012